HHS Public Access

Author manuscript

Cell Rep. Author manuscript; available in PMC 2016 April 13.

Published in final edited form as:

Cell Rep. 2015 October 13; 13(2): 376–386. doi:10.1016/j.celrep.2015.08.079.

PKA Phosphorylation of NCLX Reverses Mitochondrial Calcium Overload and Depolarization, Promoting Survival of PINK1-Deficient Dopaminergic Neurons

Marko Kostic[1,6], **Marthe H.R. Ludtmann**[2,6], **Hilmar Bading**[3], **Michal Hershfinkel**[1], **Erin Steer**[4], **Charleen T. Chu**[4,5], **Andrey Y. Abramov**[2,*], and **Israel Sekler**[1,*]

[1]Department of Physiology and Cell Biology, Faculty of Health Sciences, Ben-Gurion University of the Negev, Beer-Sheva 84105, Israel

[2]Department of Molecular Neuroscience, UCL Institute of Neurology, Queen Square, London WC1N 3BG, UK

[3]Department of Neurobiology, University of Heidelberg, Heidelberg 69120, Germany

[4]Department of Pathology, University of Pittsburgh School of Medicine, Pittsburgh, PA 15261, USA

[5]Center for Neuroscience, University of Pittsburgh School of Medicine, Pittsburgh, PA 15261, USA

SUMMARY

Mitochondrial Ca^{2+} overload is a critical, preceding event in neuronal damage encountered during neurodegenerative and ischemic insults. We found that loss of PTEN-induced putative kinase 1 (PINK1) function, implicated in Parkinson disease, inhibits the mitochondrial Na^{+}/Ca^{2+} exchanger (NCLX), leading to impaired mitochondrial Ca^{2+} extrusion. NCLX activity was, however, fully rescued by activation of the protein kinase A (PKA) pathway. We further show that PKA rescues NCLX activity by phosphorylating serine 258, a putative regulatory NCLX site. Remarkably, a constitutively active phosphomimetic mutant of NCLX ($NCLX^{S258D}$) prevents mitochondrial Ca^{2+} overload and mitochondrial depolarization in PINK1 knockout neurons, thereby enhancing neuronal survival. Our results identify an mitochondrial Ca^{2+} transport regulatory pathway that protects against mitochondrial Ca^{2+} overload. Because mitochondrial Ca^{2+} dyshomeostasis is a prominent feature of multiple disorders, the link between NCLX and PKA may offer a therapeutic target.

*Correspondence: a.abramov@ucl.ac.uk (A.Y.A.), sekler@bgu.ac.il (I.S.).

[6]Co-first author

AUTHOR CONTRIBUTIONS

M.H., C.T.C., I.S., A.Y.A., H.B., M.K., and M.H.R.L. wrote the manuscript; M.K., M.H.R.L., and E.S. performed the experiments; I.S., A.Y.A., C.T.C., and M.H. provided experimental oversight; I.S., A.Y.A., C.T.C., M.K., and M.H.R.L. designed the experiments; I.S., A.Y.A., C.T.C., M.H., M.K., and M.H.R.L. interpreted the data.

SUPPLEMENTAL INFORMATION

Supplemental Information includes Supplemental Experimental Procedures, three figures, and one table and can be found with this article online at http://dx.doi.org/10.1016/j.celrep.2015.08.079.

Graphical abstract

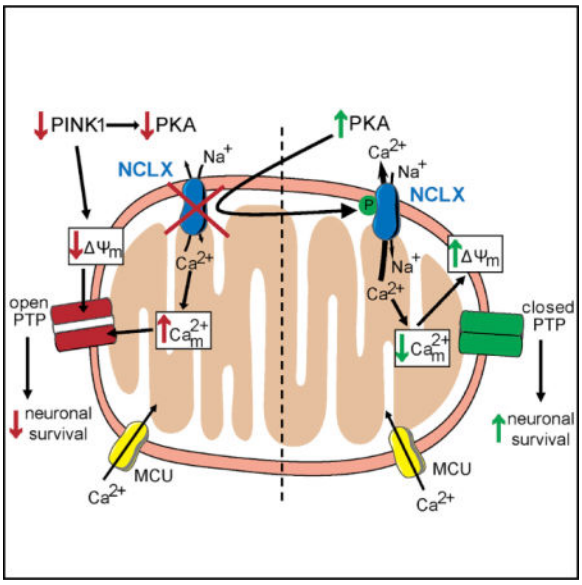

INTRODUCTION

Parkinson disease (PD) is the second most common neurodegenerative disease, characterized by a progressive loss of dopaminergic neurons in the substantia nigra pars compacta (SNc) (Barbas, 2006; Fahn, 2003). Recent discoveries show that familial forms of PD are caused by mutations in several gene products associated with mitochondrial quality control processes, reinforcing the major role of mitochondrial impairment in the pathogenesis of PD (Bogaerts et al., 2008; Dagda and Chu, 2009). One of the key models in characterizing mitochondrial pathology in PD is based on a loss of PTEN-induced putative kinase 1 (PINK1) function (Gandhi et al., 2012). PINK1 is a serine/threonine kinase localized to mitochondria that exerts a neuroprotective function, and its expression has been shown to be a Ca^{2+}-dependent process (Gómez-Sánchez et al., 2014). Loss-of-function mutations of PINK1 result in a series of mitochondrial abnormalities implicated in the etiopathology and progression of early-onset familial PD. These abnormalities include partial mitochondrial depolarization, increased oxidative stress, and mitochondrial fusion and fission defects (Valente et al., 2004; Wood-Kaczmar et al., 2008).

A hallmark of PINK1 mutations related to PD is mitochondrial calcium ($_mCa^{2+}$) overload, which renders dopaminergic neurons particularly vulnerable to injury (Gandhi et al., 2009). Adult dopaminergic neurons of the SNc are exposed to frequent and large Ca^{2+} loads, due to their autonomous pacing activity that is uniquely dependent on Ca^{2+} channels (Surmeier et al., 2012). The $_mCa^{2+}$ overload may therefore result from inability of the $_mCa^{2+}$ shuttling system to handle these loads (Chan et al., 2007). The $_mCa^{2+}$ transients in neurons are mediated by two transporters: the mitochondrial calcium uniporter (MCU), which mediates $_mCa^{2+}$ influx, and the mitochondrial Na^+/Ca^{2+} exchanger, which mediates $_mCa^{2+}$ efflux (Baughman et al., 2011; De Stefani et al., 2011; Palty et al., 2010). We have recently identified the mitochondrial Na^+/Ca^{2+} exchanger and linked it to NCLX ($Na^+/Ca^{2+}/Li^+$

exchanger), a member of the Na^+/Ca^{2+} exchanger (NCX) family of transporters that share a common catalytic core composed of α1 and α2 repeating domains (Nicoll et al., 2013; Palty et al., 2004, 2010). However, it differs markedly in the regulatory domain region, which, in contrast to other NCX members, is much shorter and lacks allosteric Ca^{2+}-binding domains (Cai and Lytton, 2004). The $_mCa^{2+}$ efflux by NCLX is much slower than the MCU-mediated $_mCa^{2+}$ influx (Drago et al., 2012). Thus, NCLX is the rate-limiting system in controlling $_mCa^{2+}$ surges (Palty et al., 2010). The profound inhibitory effect of PINK1 deficiency on $_mCa^{2+}$ removal suggests that in PD the capacity of the mitochondrial exchanger to remove $_mCa^{2+}$ is impaired. However, it is unknown whether the effects on $_mCa^{2+}$ transients are mediated through direct interaction of PINK1 with NCLX or via an indirect phenomenon, such as modulation of the $_mCa^{2+}$ influx machinery. Furthermore, it is uncertain whether impaired $_mCa^{2+}$ handling and the resulting mitochondrial depolarization and neuronal death encountered with PINK1 mutations can be rescued by other signaling pathways, such as the protein kinase A (PKA) pathway, which shows diminished activity in PINK1-deficient neuronal cells (Dagda et al., 2014).

Numerous studies support a major role of the cyclic AMP (cAMP)/PKA signaling cascade in modulating mitochondrial functions such as apoptosis, mitochondrial respiration, and ATP production (Acin-Perez et al., 2009; Martin et al., 2005; Technikova-Dobrova et al., 2001). Cyclic AMP produced by plasma membrane adenylyl cyclase can diffuse throughout the cell to set up localized gradients in subcellular organelles, including mitochondria (DiPilato et al., 2004). In addition, cAMP can be produced directly in the mitochondrial matrix by a soluble adenylyl cyclase (Chen et al., 2000). The cAMP is postulated to activate PKA, which is detected in different mitochondrial compartments (Valsecchi et al., 2013). Interestingly, PKA exhibits a prosurvival effect in PINK1-deficient cells, which is due in part to the regulation of the mitochondrial fission protein Drp1 (Dagda et al., 2011). It is, however, unknown whether the prosurvival effects of PKA are linked to modulation of $_mCa^{2+}$ signaling. Highly coordinated interplay between cAMP and Ca^{2+} signaling, which has been demonstrated in mitochondria (Di Benedetto et al., 2013), suggests the involvement of PKA in the regulation of $_mCa^{2+}$ homeostasis.

In this study, we demonstrate that NCLX activity, impaired by PINK1 deficiency, is rescued by PKA. We show that $_mCa^{2+}$ efflux occurs via direct phosphorylation of NCLX by PKA, revealing a regulatory mode of mitochondrial Na^+/Ca^{2+} exchange. Finally, we find that modulation of the NCLX phosphorylation site by PKA is essential and sufficient to protect PINK1-deficient neurons from mitochondrial depolarization and dopamine-induced cell death, underscoring the role of the exchanger and its regulation via PKA in the pathogenesis of PD and potentially in other neurodegenerative disorders of similar Ca^{2+}-dependent pathophysiology.

RESULTS

PINK1 Deficiency Causes Partial Mitochondrial Depolarization and Inhibition of $_mCa^{2+}$ Efflux

Previous studies suggested that PINK1 mutations linked to PD lead to a partial decrease in mitochondrial membrane potential (Δψm) (Abramov et al., 2011; Gandhi et al., 2009).

Another prominent feature of these mutations is susceptibility to $_{m}Ca^{2+}$ overload—a hallmark event in PD as well as other neurodegenerative and ischemic diseases (Cherra et al., 2013; Surmeier and Schumacker, 2013). We hypothesized that the pathological rise in $_{m}Ca^{2+}$ is specifically linked to impaired Ca^{2+} efflux by the mitochondrial Na^{+}/Ca^{2+} exchanger (Gandhi et al., 2009), whose molecular identity was only recently revealed (Palty et al., 2010).

We first asked whether a knockdown of PINK1 in previously characterized human neuroblastoma shPINK1 SH-SY5Y cells (Dagda et al., 2009) mirrors the lowered Δψm and impaired $_{m}Ca^{2+}$ efflux, as previously reported (Abramov et al., 2011; Gandhi et al., 2009). Δψm was recorded using the potentiometric fluorescent dye tetramethylrhodamine methyl ester (TMRM), where a complete depolarization can be induced by addition of the mitochondrial uncoupler carbonyl cyanide-*p*-trifluoromethoxyphenylhydrazone (FCCP). Basal Δψm in shPINK1 versus control cells was determined by comparing the Δψm before and after the application of FCCP. Consistent with previous findings, we recorded a significant reduction in basal Δψm in stable shPINK1 SH-SY5Y cells compared to control cells expressing a nontargeting control plasmid (64% ± 11% of control) (Figures 1A and 1B).

We next compared transient $_{m}Ca^{2+}$ responses in shPINK1 SH-SY5Y to those in control cells by using the $_{m}Ca^{2+}$ fluorescent dye Rhod-2 AM. Application of the P2Y receptor activator, ATP, triggered cytosolic followed by $_{m}Ca^{2+}$ transients (Palty et al., 2010) (Figure 1C). Consistent with a drop in Δψm —the major driving force for $_{m}Ca^{2+}$ uptake via MCU—the rate of $_{m}Ca^{2+}$ influx was reduced by ~2-fold in shPINK1 cells in comparison to control cells (Figures 1C and 1D). However, the amplitude of the $_{m}Ca^{2+}$ influx phase remained unchanged (Figures 1C and 1E), showing that, although conducted at a slightly slower rate, the capacity of mitochondria to take up Ca^{2+} remains intact. In addition, no significant difference was observed in basal $_{m}Ca^{2+}$ levels between control and PINK1-deficient cells (Figure S1).

A much stronger effect of PINK1 knockdown was, however, observed on the $_{m}Ca^{2+}$ efflux phase, as it triggered an ~3.5-fold decrease in $_{m}Ca^{2+}$ efflux rate compared to control (Figures 1C and 1F). Moreover, this reduction in $_{m}Ca^{2+}$ efflux rate was coupled to an ~4-fold reduction in the amplitude of the $_{m}Ca^{2+}$ efflux phase (Figures 1C and 1G). Hence, whereas Ca^{2+} efflux fully recovered the $_{m}Ca^{2+}$ to resting levels in control cells, mitochondria of PINK1-deficient cells, in contrast, failed to effectively extrude Ca^{2+} and it remained elevated above resting levels. Taken together, our results, consistent with previous studies, suggested that PINK1 deficiency reduces $_{m}Ca^{2+}$ uptake (Gandhi et al., 2009; Heeman et al., 2011) but has a larger effect on both the rate and amplitude of the $_{m}Ca^{2+}$ efflux phase, thereby triggering a net reduction in $_{m}Ca^{2+}$ extrusion.

We next determined whether PINK1 knockdown caused changes in expression of NCLX in shPINK1 versus control cells. Immunoblot analysis of shPINK1 cells showed similar levels of NCLX expression compared to control cells (Figures 1H and 1I), indicating that overload of $_{m}Ca^{2+}$ is not caused by a decrease in NCLX expression but is most likely due to inhibition of NCLX activity in PINK1-deficient cells.

The profound effect of shPINK1 on $_{m}Ca^{2+}$ efflux suggests that this kinase may act by directly interacting with the exchanger, NCLX. Bioinformatic analysis that we conducted using the Scansite algorithm (Obenauer et al., 2003), however, did not identify potential PINK1 binding or phosphorylation sites on NCLX. Consistent with this analysis and previous study that did not identify NCLX interaction with PINK1 (Rakovic et al., 2011), immunoprecipitation of c-*myc*-tagged NCLX followed by mass spectrometry (MS) analysis did not identify a pull-down of PINK1 by NCLX (Table S1), arguing against a direct interaction between these two proteins.

PKA Activation Rescues $_{m}Ca^{2+}$ Efflux and Mitochondrial Membrane Depolarization Triggered by PINK1 Deficiency

We next sought to determine whether we could rescue $_{m}Ca^{2+}$ efflux of PINK1-deficient SH-SY5Y cells. Because the above results do not support a direct interaction of PINK1 and NCLX, we reasoned that such rescue of NCLX activity may be mediated by another signaling pathway. Among the potential signaling pathways the PKA pathway emerged as a leading signaling candidate able to rescue several parameters of PINK1 deficiency, most notably $\Delta\psi m$ (Dagda et al., 2011). To determine whether PKA regulates NCLX activity, we monitored $_{m}Ca^{2+}$ transients and $\Delta\psi m$ in PINK1-deficient SH-SY5Y cells versus control cells that were pre-exposed to the PKA agonist forskolin. Application of forskolin led to a full recovery of $\Delta\psi m$ in shPINK1 cells up to the control values, but was not followed by a change in $\Delta\psi m$ of control cells (Figures 2A and 2B).

Consistent with the role of $\Delta\psi m$ in controlling the driving force for $_{m}Ca^{2+}$ influx, $\Delta\psi m$ rescue by PKA activation was followed by recovery of $_{m}Ca^{2+}$ influx rates in shPINK1 SH-SY5Y cells (Figures 2C and 2D). Importantly, activation of PKA further led to a much stronger, ~6-fold increase in $_{m}Ca^{2+}$ efflux rate in shPINK1 SH-SY5Y cells, thereby fully restoring $_{m}Ca^{2+}$ efflux to rates monitored in control cells (Figures 2C and 2E). We also found that application of forskolin could enhance, to a lesser extent, by ~2-fold, the rate of $_{m}Ca^{2+}$ efflux but not $_{m}Ca^{2+}$ influx of control cells, thus supporting a role of PKA in regulating NCLX rather than MCU (Figures 2D and 2E). To further ascertain that forskolin acts via PKA, cells were cotreated with forskolin and the PKA inhibitor H89. Note that their coapplication completely abolished $_{m}Ca^{2+}$ efflux activation, both in shPINK1 and control cells (Figures 2D and 2E), lending further support that the effect of forskolin on NCLX is mediated via PKA.

Serine 258 Is the Putative PKA Phosphorylation Site of NCLX

PKA can regulate NCLX indirectly through other signaling pathways or by direct phosphorylation of the exchanger. To determine whether PKA acts directly on NCLX, we screened for putative PKA phosphorylation sites employing the Scansite 3 algorithm. A high score of probability was given to serine residue 258 (S258). The potential of S258 to undergo PKA-dependent phosphorylation was further supported by NetPhosK 1.0 (Blom et al., 2004) and pkaPS analysis (Neuberger et al., 2007), which indicated that S258 is part of a PKA signature sequence, RRXSY (where Y is a hydrophobic amino acid, leucine in this case). Figure 3A shows the predicted transmembrane topology model of NCLX depicting the putative S258 PKA phosphorylation site. This putative phosphorylation site is located

within the hydrophilic loop of the exchanger, which in other NCX superfamily members serves as the major regulatory site responding to allosterically bound Ca^{2+} (the so-called CBD1 and CBD 2) (Nicoll et al., 2013). NCLX is devoid of these Ca^{2+} binding sites, but has instead the putative PKA phosphorylation site at this domain.

To examine whether S258 indeed undergoes phosphorylation, and whether it is phosphorylated in a PKA-dependent manner, we employed MS analysis of c-*myc*-tagged NCLX treated with forskolin, with or without H89, as described in Figure 2. MS analysis identified phosphorylation of S258 in forskolin-treated but not H89-cotreated NCLX (Figure 3B). Furthermore, in vitro analysis of immunopurified NCLX revealed that S258 is phosphorylated in the presence of the PKA catalytic subunit as well, supporting direct phosphorylation of NCLX by PKA (Figure 3B).

To further determine whether phosphorylation at S258 could explain the functional effects of PKA on NCLX activity, we generated $NCLX^{S258A}$ and $NCLX^{S258D}$ mutants to mimic phosphorylation-deficient and constitutively phosphorylated residues, respectively. To ascertain that the mutation did not affect the expression or localization of NCLX, we employed immunoblot analysis of expression in total and mitochondrial cell fractions. As shown in Figure 3C, the expression and localization of the mutants were similar to that of $NCLX^{WT}$.

We next monitored $_{m}Ca^{2+}$ efflux activity of the NCLX mutants versus $NCLX^{WT}$ by applying a silencing-rescue paradigm (Palty et al., 2010) of knocking down endogenous NCLX expression while expressing NCLX constructs in cells coexpressing the $_{m}Ca^{2+}$ sensor mito-Pericam. Consistent with our previous studies (Palty et al., 2010), silencing of endogenous NCLX expression in HEK293T cells, using small hairpin RNA (shRNA) targeted against the 3′ UTR of NCLX, was followed by an ~2.5-fold reduction in $_{m}Ca^{2+}$ efflux rates compared to cells transfected with control shRNA, which was fully rescued by overexpression of $NCLX^{WT}$ (Figure S2A).

Similar to $NCLX^{WT}$, phosphomimicking mutant $NCLX^{S258D}$ was able to fully rescue $_{m}Ca^{2+}$ efflux in shNCLX-treated cells. On the contrary, phosphodeficient mutant $NCLX^{S258A}$ failed to upregulate $_{m}Ca^{2+}$ efflux, with an ~3.5-fold decrease in activity compared to $NCLX^{S258D}$ (Figures 3 D and 3E). In addition, no difference in basal $_{m}Ca^{2+}$ levels was observed between the mutants and $NCLX^{WT}$ (Figure S2B).

The difference in activity between $NCLX^{S258A}$ and $NCLX^{S258D}$ mutants was further confirmed, applying the same silencing-rescue paradigm (Palty et al., 2010), in digitonin-permeabilized HEK293T cells. The mitochondria of permeabilized HEK293T cells transiently expressing mito-Pericam and shNCLX, alone or in a combination with NCLX constructs, were loaded with Ca^{2+}, and Ca^{2+} efflux was initiated by addition of Na^{+}, in the presence of the MCU blocker Ruthenium red, as previously described (Palty et al., 2010). Consistent with our finding in intact cells, silencing of endogenous NCLX profoundly inhibited the Na^{+}-dependent Ca^{2+} efflux, which was fully rescued by overexpression of either $NCLX^{S258D}$ or $NCLX^{WT}$ (Figures 3F and 3G; Figure S2C). In contrast, the

NCLX^{S258A} mutant, although demonstrating some residual activity, was inhibited by more than 2-fold compared to either NCLX^{S258D} or NCLX^{WT} (Figures 3F and 3G).

Taken together, these results indicate that phosphorylation at S258 mediates the effects of PKA on $_{m}Ca^{2+}$ efflux.

Expression of Phosphomimetic NCLX^{S258D}, but Not Phosphodeficient NCLX^{S258A}, Suppresses the Inhibitory Effect of PINK1 Deficiency on $_{m}Ca^{2+}$ Efflux

If the S258 residue is the critical site regulated by PKA, then expressing the constitutively active NCLX^{S258D} or the inactive NCLX^{S258A} mutant is expected to eliminate, in both cases, the responsiveness to forskolin that we observed for the endogenous NCLX (Figures 2C and 2E). Consistent with previous findings, we confirmed that NCLX^{WT} is responsive to PKA activation and activates by ~2-fold when treated with forskolin (Figures 4A and 4B). On the other hand, activity of NCLX^{S258A} in the presence of forskolin remained low and that of NCLX^{S258D} was constitutively high, in agreement with their inactivation and activation phenotypes, respectively (Figures 4A and 4B).

If phosphorylation of NCLX at the PKA site, S258, is required for activation of $_{m}Ca^{2+}$ efflux, NCLX^{S258D} should remain activated compared to NCLX^{S258A} when expressed in shPINK1 SH-SY5Y cells. Indeed, $_{m}Ca^{2+}$ efflux rates of shPINK1 SH-SY5Y cells expressing phosphomimetic mutant NCLX^{S258D} were almost 2-fold higher than the rates recorded in cells expressing phosphodeficient NCLX^{S258A} (Figures 4C and 4D). Note that NCLX^{WT} was also active in shPINK1 cells, indicating that the residual PKA activity observed in these cells is sufficient to activate NCLX, consistent with the critical role of intact S258 for its activation, and further showing that higher heterologous expression of NCLX^{WT} can compensate for lesser PKA activity. Thus, modulation of the S258 site is essential and sufficient to fully recover $_{m}Ca^{2+}$ efflux rates from the inhibitory effect observed in PINK1-deficient SH-SY5Y cells.

NCLX Phosphomimetics Also Rescues $_{m}Ca^{2+}$ Overload in PINK1 Knockout Neurons

To determine the effect of the NCLX mutants in PINK1 knockout (KO) mouse neurons, intact neurons were loaded with the Ca^{2+} indicator X-Rhod-1 and $_{m}Ca^{2+}$ was assessed upon provision of a physiological stimulus (Figure 5A). It should be noted that X-Rhod-1 labels mitochondrial as well as cytosolic Ca^{2+}. However, only mitochondrial areas were selected for analysis (Figure S3). We stimulated either WT or PINK1 KO neurons with 1 μM glutamate, which caused a transient increase in cytosolic Ca^{2+}, followed by changes in $_{m}Ca^{2+}$, as mitochondria buffer this surge in cytosolic Ca^{2+} (Figure 5B). PINK1 KO cells displayed a markedly reduced $_{m}Ca^{2+}$ efflux rate, by ~10-fold compared to WT neurons (Figures 5C and 5D). However, mitochondria of PINK1 KO cells overexpressing NCLX^{S258D} and NCLX^{WT} displayed faster Ca^{2+} exclusion rates, similar to those observed in WT neurons (Figures 5C and 5D). In contrast, overexpression of NCLX^{S258A} failed to rescue the aberrant $_{m}Ca^{2+}$ efflux in PINK1 KO neurons (Figures 5C and 5D).

To eliminate any differences in $_{m}Ca^{2+}$ handling due to varying cytosolic Ca^{2+} responses, cells were permeabilized in pseudointracellular medium after X-Rhod-1 loading. Permeabilization of neurons allowed for precise control over Ca^{2+} concentrations outside of

the mitochondria and direct measurement of $_{m}Ca^{2+}$ handling (Figure 5E). Application of 5 μM Ca^{2+} led to a transient increase and exclusion of $_{m}Ca^{2+}$ within 0.5–1 min in WT cells (Figures 5F and 5G). In agreement with previous data (Abramov et al., 2011; Gandhi et al., 2009), deletion of PINK1 led to altered $_{m}Ca^{2+}$ efflux, mirroring that observed in whole-cell experiments (Figures 5F and 5G). Similar to our results in intact PINK1 KO neurons, overexpression of $NCLX^{S258D}$ or $NCLX^{WT}$ rescued the $_{m}Ca^{2+}$ efflux in permeabilized neurons when compared to either PINK1 KO or PINK1 KO $NCLX^{S258A}$-expressing cells (Figures 5F and 5G).

Mitochondrial Membrane Potential Is Rescued through Overexpression of $NCLX^{S258D}$ but Not of the $NCLX^{S258A}$ Mutant

Normalization of Δψm in PINK1 KO cells by pyruvate and succinate did not change the inhibited Na^{+}/Ca^{2+} exchange in these cells (Gandhi et al., 2009), suggesting that it is not the most upstream mechanism by which PINK1 deficiency affects $_{m}Ca^{2+}$ efflux. Because excess mitochondrial matrix Ca^{2+} can trigger the loss of membrane potential (Vergun and Reynolds, 2005), we studied whether a recovery of $_{m}Ca^{2+}$ efflux via PKA-mediated activation of NCLX could lead to a rescue of Δψm in PINK1 KO neurons.

As expected, PINK1 KO neurons possessed significantly reduced Δψm (77% ± 5% of WT control) (Figure 6A). We first checked whether PKA activation by forskolin can suppress this reduction in Δψm. Similar to the effect observed in PINK1-deficient SH-SY5Y cells (Figures 2A and 2B), we observed a full rescue of Δψm in PINK1 KO neurons in the presence of forskolin (Figure 6A).

We then asked whether expression of phosphomimetic $NCLX^{S258D}$ or $NCLX^{WT}$ could recover Δψm in PINK1 KO neurons. Notably, overexpression of $NCLX^{S258D}$ and $NCLX^{WT}$ restored Δψm in PINK1 KO cells back to its level in WT neurons (104% ± 8% and 110% ± 12% of WT control, respectively) (Figure 6B). In contrast, $NCLX^{S258A}$ expression in PINK1 KO failed to restore the Δψm (72% ± 5% of WT control) (Figure 6B).

$NCLX^{S258D}$ but Not $NCLX^{S258A}$ Overexpression Protects PINK1 KO Neurons from Dopamine-Induced Cell Death

The $_{m}Ca^{2+}$ dysregulation and overload can trigger premature opening of the mitochondrial permeability transition pore (mPTP) and cell death (Crompton, 1999; Nicholls and Budd, 2000). We reasoned that, by rescuing both $_{m}Ca^{2+}$ efflux and Δψm, phosphomimicking mutant $NCLX^{S258D}$, but not $NCLX^{S258A}$, should prevent the opening of mPTP and increase neuronal survival of PINK1 KO neurons. PINK1 KO cells are prone to dopamine-induced cell toxicity, and incubation of PINK1 KO midbrain cultures with 50 μM dopamine triggered cell death (73% ± 3%), which was significantly higher compared to control PINK1 KO neurons not treated with dopamine (3% ± 1%), consistent with previous results (Gandhi et al., 2012) (Figure 6C). In accordance with our hypothesis, expression of $NCLX^{S258A}$ failed to have an effect (66% ± 2%), whereas expression of both $NCLX^{S258D}$ and $NCLX^{WT}$ significantly reduced dopamine-induced cell death of PINK1 KO neurons (49% ± 4% and 45% ± 3, respectively) (Figure 6C).

DISCUSSION

Loss-of-function mutations of PINK1, a mitochondrially targeted serine/threonine kinase, are linked to recessively inherited PD (Gandhi et al., 2009; Valente et al., 2004). A major hallmark of PINK1 deficiency in neurons is an $_{m}Ca^{2+}$ overload, which leads to neuronal cell death triggered by the opening of mPTP (Abramov et al., 2011; Akundi et al., 2011; Gandhi et al., 2009; Gautier et al., 2008). Previous findings suggested that the $_{m}Ca^{2+}$ overload related to the loss of PINK1 occurs due to specific inhibition of $_{m}Ca^{2+}$ efflux from dopaminergic neurons (Gandhi et al., 2009). The prevailing route of Ca^{2+} efflux from neuronal mitochondria is its exchange with Na^{+} via the mitochondrial Na^{+}/Ca^{2+} exchanger NCLX (Gunter et al., 2000). Loss of PINK1, however, strongly inhibits exchange activity, as neither $_{m}Ca^{2+}$ removal nor concomitant mitochondrial Na^{+} influx is observed upon triggering $_{m}Ca^{2+}$ influx in PINK1 KO neurons (Gandhi et al., 2009). Here we confirm that the $_{m}Ca^{2+}$ efflux is significantly reduced in PINK1 KO mouse dopaminergic neurons and, furthermore, we demonstrate a similar inhibition of $_{m}Ca^{2+}$ efflux by stably knocking down PINK1 in a human neuroblastoma cell line (SH-SY5Y). The inhibition of $_{m}Ca^{2+}$ efflux could be mediated either by a direct interaction/phosphorylation of PINK1 with NCLX or by an indirect effect of PINK1 loss that communicates with NCLX through a distinct pathway (Figure 7). The following results argue against a direct interaction of NCLX and PINK1: (1) bioinformatic analysis failed to identify any PINK1 phosphorylation site on NCLX; (2) proteomic analysis of PINK1-interacting proteins found 14 candidates, but NCLX was not among them (Rakovic et al., 2011); and (3) our MS analysis of overexpressed NCLX failed to identify interaction with PINK1 or phosphorylation of NCLX related to this kinase (Table S1).

Recent studies, however, indicate that loss of PINK1 leads to PKA inhibition (Dagda et al., 2014). We show that PKA strongly modulates $_{m}Ca^{2+}$ efflux. This effect can be mediated indirectly or by PKA-dependent phosphorylation of NCLX. The following results support the latter mechanism. (1) The inclusion of a PKA inhibitor abolished the forskolin-dependent upregulation of NCLX activity. Our findings are consistent with early studies demonstrating a cAMP-dependent upregulation of Na^{+}-dependent $_{m}Ca^{2+}$ efflux (Goldstone and Crompton, 1982). (2) NCLX harbors a potential PKA phosphorylation site at S258, which we now show by MS analysis is phosphorylated by activation of PKA in cells and directly by PKA in an in vitro purified NCLX preparation (Figure 3B). Importantly, when S258 is replaced by aspartate ($NCLX^{S258D}$), $_{m}Ca^{2+}$ efflux by NCLX is enhanced, whereas changing it to alanine ($NCLX^{S258A}$) downregulates $_{m}Ca^{2+}$ efflux. (3) The activity of $NCLX^{S258D}$ and $NCLX^{S258A}$ is nonresponsive to the PKA agonist, indicating that S258 is indeed the target site for PKA on NCLX (Figure 7). The S258 residue of NCLX is described here as a regulatory switch in this exchanger, and phosphorylation at this site represents a mode of regulation for mitochondrial Na^{+}/Ca^{2+} exchange. Furthermore, our results indicate that mimicking phosphorylation of S258 plays a key role in preventing $_{m}Ca^{2+}$ overload in several injury paradigms, and may therefore be an attractive therapeutic target. Notably, overexpression of $NCLX^{WT}$ can also overcome the downregulation of NCLX activity in PINK1-deficient cells. This finding is consistent with the partial inhibition of PKA following PINK1 knockdown (Dagda et al., 2014). Thus, overexpression of $NCLX^{WT}$ may

increase the availability of the regulatory site to PKA. Indeed, overexpression of the inactive $NCLX^{S258A}$ failed to produce a similar activation, strongly supporting the regulatory importance of this site (Figure 7).

Plasma membrane NCXs possess a regulatory mechanism involving cytosolic Ca^{2+} that is well defined. NCX has a long intracellular loop that carries two Ca^{2+}-binding domains (CBD1 and CBD2) that strongly and allosterically regulate NCX following changes in cytosolic Ca^{2+} (Nicoll et al., 2013). However, the homologous hydrophilic loop of NCLX is much shorter and lacks any obvious Ca^{2+}-binding domains. In contrast, it possesses the PKA phosphorylation site defined in the current study. Our results therefore indicate that NCLX has an entirely different mode of regulation compared to the plasma membrane NCXs—it is based on phosphorylation, not on allosteric Ca^{2+} binding.

Two distinct pools of cAMP/PKA signaling mediators are capable of reaching and regulating mitochondria. The first is associated with cytosolic cAMP that is produced by cell membrane adenylyl cyclase, which can activate PKA, allowing it to translocate to the outer mitochondrial membrane and intermembrane space (Lefkimmiatis et al., 2013). The second is generated by a soluble adenylyl cyclase that is solely contained in the mitochondrial matrix (Acin-Perez et al., 2009; Di Benedetto et al., 2013). Although the sensitivity of cytosolic PKA to forskolin suggests its role in NCLX regulation, further studies are required to determine the subcellular origin of PKA species that participate in NCLX regulation.

Another distinctive aspect of PINK1 deficiency in neurons is a partial mitochondrial depolarization, which significantly contributes to the increased neuronal death related to PINK1 loss (Abramov et al., 2011; Dagda et al., 2011). The reduced $\Delta\psi m$ in PINK1 KO neurons can be restored by provision of substrates of mitochondrial respiratory chain complexes I and II. However, this rescue of $\Delta\psi m$ does not recover $_{m}Ca^{2+}$ efflux deficits, suggesting that the inhibition of the exchanger is upstream of the mitochondrial depolarization. Here we demonstrate that $_{m}Ca^{2+}$ efflux can be fully reconstituted by expression of constitutively active mutant $NCLX^{S258D}$, which furthermore fully rescues $\Delta\psi m$ in PINK1 KO neurons. These results imply that the impairment of $_{m}Ca^{2+}$ shuttling is due to diminished NCLX activity encountered in PINK1 deficiency, which in turn contributes, at least in part, to the mitochondrial depolarization.

Interestingly, we previously found that PINK1-deficient cells exhibit reduced PKA signaling (Dagda et al., 2014). Although it is possible that the two pathways operate in parallel, PINK1 and PKA exhibit features of a positive amplifying interaction. Loss of PINK1 selectively suppresses the ability of cAMP, but not retinoic acid, to induce neuronal differentiation (Dagda et al., 2014). This is accompanied by decreased indices of PKA activity (CRE-luciferase and CREB phosphorylation) in PINK1 shRNA cells (Dagda et al., 2014). Conversely, PINK1 overexpression elevates CRE activity and enhances neurite outgrowth; these effects of PINK1 are inhibited by H89 or expression of a mitochondrially targeted peptide inhibitor of PKA (Dagda et al., 2014). These data suggest that PINK1 is necessary for full activity of PKA at the mitochondrion. Thus, the reduction in NCLX activity observed in PINK1-deficient cells and neurons could be due to reduced PKA activation in these cells (Figure 7). Although it is possible that PINK1 deficiency also affects

other parallel pathways, our current results clearly indicate that PKA-mediated upregulation of NCLX activity can break these vicious cycles in PINK1-deficient neurons to rescue not only the $_{m}Ca^{2+}$ overload but also the $\Delta\psi m$ (Figure 7).

One would expect that by rescuing both $_{m}Ca^{2+}$ efflux and $\Delta\psi m$, expression of the constitutively active exchanger $NCLX^{S258D}$ would result in reduced neuronal cell death related to PINK1 deficiency. Indeed, we recorded a significant increase in neuronal survival rate upon expression of $NCLX^{S258D}$ or $NCLX^{WT}$, but not $NCLX^{S258A}$, implying that modulation of the NCLX phosphorylation site by PKA activation is essential and sufficient to protect PINK1-deficient neurons from dopamine-induced cell death. Taken together, our results establish NCLX as the major player implicated in several mitochondrial defects related to PD caused by PINK1 impairment.

Mitochondria play a major role in the regulation of cellular Ca^{2+} homeostasis (De Smedt et al., 2011). Impairment of $_{m}Ca^{2+}$ shuttling results in $_{m}Ca^{2+}$ overload similar to that related to PINK1 deficiency, which is implicated in a range of neurodegenerative and ischemic diseases. This notion further highlights the importance of the exchanger and the regulatory mechanism via PKA described in this paper. Under physiological conditions in the steady state, NCLX and MCU Ca^{2+} transport must be in balance. Under pathophysiological conditions, however, $_{m}Ca^{2+}$ overload can occur either as a result of increased $_{m}Ca^{2+}$ uptake via MCU or reduced $_{m}Ca^{2+}$ removal via NCLX, as observed in PINK1-deficient cells (Gandhi et al., 2009). In the latter case, activation of NCLX via the PKA regulatory pathway leads to a recovery of impaired $_{m}Ca^{2+}$ handling and neuronal rescue (Figure 7), which opens new avenues for future targeted therapeutic strategies for these disorders.

EXPERIMENTAL PROCEDURES

Mice

Wild-type and PINK1 KO mice were from breeding colonies generated by Lexicon Genetics. Animal breeding and maintenance were in accordance with the regulations described in UK Animals (Scientific Procedures) Act 1986.

Cell Culture and Transfection

HEK293T cells were as previously described (Palty et al., 2004). Stable PINK1 shRNA knockdown SH-SY5Y cell lines were generated and cultured as previously described (Dagda et al., 2009). Primary midbrain mouse neurons were isolated and cultured as previously described (Gandhi et al., 2009). Transfection of HEK293T cells was performed using the calcium phosphate precipitation protocol as previously described (Palty et al., 2004). SH-SY5Y cells and primary neuronal cells were transfected using Lipofectamine 2000 (Invitrogen) and Effectine (QIAGEN), respectively, according to the manufacturers' protocols.

Immunoblot Analysis

NCLX and PINK1 immunoblotting was performed as previously reported (Palty et al., 2010). For specific determination of NCLX expression in mitochondria, cell fractionation

was performed as previously described (Bozidis et al., 2007). Immunoblot analysis was performed as described previously (Palty et al., 2010) using the following antibodies: custom-made antibody against NCLX (Palty et al., 2004; 1:1,000), rabbit polyclonal anti-PINK1 antibody (Abcam; 1:200), anti-β-actin (Sigma; 1:20,000), and anti-cytochrome *c* oxidase (COXIV-1) antibody (Santa Cruz Biotechnology; 1:100).

Immunoprecipitation and MS Analysis

HEK293T cells were transfected with a c-*myc*-tagged human NCLX-encoding plasmid. Forty-eight hours posttransfection, cells were incubated with forskolin or cotreated with H89 and forskolin and then lysed in the presence of protease inhibitors (Sigma) and phosphatase inhibitors (PhosSTOP; Roche), and the lysate was immunoprecipitated with anti-c-*myc* agarose beads (Pierce Anti-c-Myc agarose; Thermo Scientific) using the manufacturer's protocol. On-bead tryptic proteolysis and MS were performed as previously described (Fukuyama et al., 2012).

Fluorescent Ca^{2+} and $\Delta\psi m$ Imaging

In HEK293T cells, the $_{m}Ca^{2+}$ levels were monitored by transiently expressed mitochondrially targeted ratiometric Pericam (mito-Pericam) as previously described (Palty et al., 2010). The m $_{m}Ca^{2+}$ measurement in SH-SY5Y cells was performed using Rhod-2 AM fluorescent Ca^{2+} dye as previously described (Jaiswal et al., 2009). Changes in inner $\Delta\psi m$ were monitored using TMRM as previously described (Nita et al., 2012).

Confocal Imaging

Confocal images of X-Rhod-1-loaded neurons were obtained as previously described (Gandhi et al., 2009).

Toxicity Experiments

For toxicity assays, we loaded cells simultaneously with 20 μM propidium iodide, which is excluded from viable cells but exhibits a red fluorescence following a loss of membrane integrity, and 4.5 μM Hoechst 33342 (Molecular Probes), which gives a blue staining to chromatin, to count the total number of cells.

Statistical Analysis

All results are presented as mean ± SEM. Statistical significance was determined using t test or one-way ANOVA test followed by Tukey post hoc analysis. Values of $p < 0.05$ were considered significant.

Supplementary Material

Refer to Web version on PubMed Central for supplementary material.

Acknowledgments

This study was supported by Israel Science Foundation (ISF) and German-Israeli Project Cooperation (DIP) grants (SE 2372/1-1; to I.S., M.H., and H.B.), an NIHR Biomedical Research Centres funding streams grant (to A.Y.A.), and NIH R01 NS065789 (to C.T.C.). We would like to thank Dr. Tevie Mehlman from the Weizmann Institute of

Science for MS analysis, Dr. Tsipi Ben Kasus from Ben Gurion University for the generation of NCLX mutants, and Dr. Soumitra Roy for the experiments with HEK293T permeabilized cells.

References

Abramov AY, Gegg M, Grunewald A, Wood NW, Klein C, Schapira AH. Bioenergetic consequences of PINK1 mutations in Parkinson disease. PLoS ONE. 2011; 6:e25622. [PubMed: 22043288]

Acin-Perez R, Salazar E, Kamenetsky M, Buck J, Levin LR, Manfredi G. Cyclic AMP produced inside mitochondria regulates oxidative phosphorylation. Cell Metab. 2009; 9:265–276. [PubMed: 19254571]

Akundi RS, Huang Z, Eason J, Pandya JD, Zhi L, Cass WA, Sullivan PG, Büeler H. Increased mitochondrial calcium sensitivity and abnormal expression of innate immunity genes precede dopaminergic defects in Pink1-deficient mice. PLoS ONE. 2011; 6:e16038. [PubMed: 21249202]

Barbas NR. Cognitive, affective, and psychiatric features of Parkinson's disease. Clin Geriatr Med. 2006; 22:773–796. v–vi. [PubMed: 17000335]

Baughman JM, Perocchi F, Girgis HS, Plovanich M, Belcher-Timme CA, Sancak Y, Bao XR, Strittmatter L, Goldberger O, Bogorad RL, et al. Integrative genomics identifies MCU as an essential component of the mitochondrial calcium uniporter. Nature. 2011; 476:341–345. [PubMed: 21685886]

Blom N, Sicheritz-Ponten T, Gupta R, Gammeltoft S, Brunak S. Prediction of post-translational glycosylation and phosphorylation of proteins from the amino acid sequence. Proteomics. 2004; 4:1633–1649. [PubMed: 15174133]

Bogaerts V, Theuns J, van Broeckhoven C. Genetic findings in Parkinson's disease and translation into treatment: a leading role for mitochondria? Genes Brain Behav. 2008; 7:129–151. [PubMed: 17680806]

Bozidis P, Williamson CD, Colberg-Poley AM. Isolation of endoplasmic reticulum, mitochondria, and mitochondria-associated membrane fractions from transfected cells and from human cytomegalovirus-infected primary fibroblasts. Curr Protoc Cell Biol. 2007 *Chapter 3*, Unit 3.27.

Cai X, Lytton J. Molecular cloning of a sixth member of the K^+-dependent Na^+/Ca^{2+} exchanger gene family, NCKX6. J Biol Chem. 2004; 279:5867–5876. [PubMed: 14625281]

Chan CS, Guzman JN, Ilijic E, Mercer JN, Rick C, Tkatch T, Meredith GE, Surmeier DJ. 'Rejuvenation' protects neurons in mouse models of Parkinson's disease. Nature. 2007; 447:1081–1086. [PubMed: 17558391]

Chen Y, Cann MJ, Litvin TN, Iourgenko V, Sinclair ML, Levin LR, Buck J. Soluble adenylyl cyclase as an evolutionarily conserved bicarbonate sensor. Science. 2000; 289:625–628. [PubMed: 10915626]

Cherra SJ III, Steer E, Gusdon AM, Kiselyov K, Chu CT. Mutant LRRK2 elicits calcium imbalance and depletion of dendritic mitochondria in neurons. Am J Pathol. 2013; 182:474–484. [PubMed: 23231918]

Crompton M. The mitochondrial permeability transition pore and its role in cell death. Biochem J. 1999; 341:233–249. [PubMed: 10393078]

Dagda RK, Chu CT. Mitochondrial quality control: insights on how Parkinson's disease related genes PINK1, parkin, and Omi/HtrA2 interact to maintain mitochondrial homeostasis. J Bioenerg Biomembr. 2009; 41:473–479. [PubMed: 20012177]

Dagda RK, Cherra SJ III, Kulich SM, Tandon A, Park D, Chu CT. Loss of PINK1 function promotes mitophagy through effects on oxidative stress and mitochondrial fission. J Biol Chem. 2009; 284:13843–13855. [PubMed: 19279012]

Dagda RK, Gusdon AM, Pien I, Strack S, Green S, Li C, Van Houten B, Cherra SJ III, Chu CT. Mitochondrially localized PKA reverses mitochondrial pathology and dysfunction in a cellular model of Parkinson's disease. Cell Death Differ. 2011; 18:1914–1923. [PubMed: 21637291]

Dagda RK, Pien I, Wang R, Zhu J, Wang KZ, Callio J, Banerjee TD, Dagda RY, Chu CT. Beyond the mitochondrion: cytosolic PINK1 remodels dendrites through protein kinase A. J Neurochem. 2014; 128:864–877. [PubMed: 24151868]

De Smedt H, Verkhratsky A, Muallem S. Ca(2+) signaling mechanisms of cell survival and cell death: an introduction. Cell Calcium. 2011; 50:207–210. [PubMed: 21741085]

De Stefani D, Raffaello A, Teardo E, Szabò I, Rizzuto R. A forty-kilodalton protein of the inner membrane is the mitochondrial calcium uniporter. Nature. 2011; 476:336–340. [PubMed: 21685888]

Di Benedetto G, Scalzotto E, Mongillo M, Pozzan T. Mitochondrial Ca^{2+} uptake induces cyclic AMP generation in the matrix and modulates organelle ATP levels. Cell Metab. 2013; 17:965–975. [PubMed: 23747252]

DiPilato LM, Cheng X, Zhang J. Fluorescent indicators of cAMP and Epac activation reveal differential dynamics of cAMP signaling within discrete subcellular compartments. Proc Natl Acad Sci USA. 2004; 101:16513–16518. [PubMed: 15545605]

Drago I, De Stefani D, Rizzuto R, Pozzan T. Mitochondrial Ca^{2+} uptake contributes to buffering cytoplasmic Ca^{2+} peaks in cardiomyocytes. Proc Natl Acad Sci USA. 2012; 109:12986–12991. [PubMed: 22822213]

Fahn S. Description of Parkinson's disease as a clinical syndrome. Ann N Y Acad Sci. 2003; 991:1–14. [PubMed: 12846969]

Fukuyama H, Ndiaye S, Hoffmann J, Rossier J, Liuu S, Vinh J, Verdier Y. On-bead tryptic proteolysis: an attractive procedure for LC-MS/ MS analysis of the *Drosophila* caspase 8 protein complex during immune response against bacteria. J Proteomics. 2012; 75:4610–4619. [PubMed: 22450469]

Gandhi S, Wood-Kaczmar A, Yao Z, Plun-Favreau H, Deas E, Klupsch K, Downward J, Latchman DS, Tabrizi SJ, Wood NW, et al. PINK1-associated Parkinson's disease is caused by neuronal vulnerability to calcium-induced cell death. Mol Cell. 2009; 33:627–638. [PubMed: 19285945]

Gandhi S, Vaarmann A, Yao Z, Duchen MR, Wood NW, Abramov AY. Dopamine induced neurodegeneration in a PINK1 model of Parkinson's disease. PLoS ONE. 2012; 7:e37564. [PubMed: 22662171]

Gautier CA, Kitada T, Shen J. Loss of PINK1 causes mitochondrial functional defects and increased sensitivity to oxidative stress. Proc Natl Acad Sci USA. 2008; 105:11364–11369. [PubMed: 18687901]

Goldstone TP, Crompton M. Evidence for beta-adrenergic activation of Na^{+}-dependent efflux of Ca^{2+} from isolated liver mitochondria. Biochem J. 1982; 204:369–371. [PubMed: 7115328]

Gómez-Sánchez R, Gegg ME, Bravo-San Pedro JM, Niso-Santano M, Alvarez-Erviti L, Pizarro-Estrella E, Gutiérrez-Martín Y, Alvarez-Barrientos A, Fuentes JM, González-Polo RA, Schapira AH. Mitochondrial impairment increases FL-PINK1 levels by calcium-dependent gene expression. Neurobiol Dis. 2014; 62:426–440. [PubMed: 24184327]

Gunter TE, Buntinas L, Sparagna G, Eliseev R, Gunter K. Mitochondrial calcium transport: mechanisms and functions. Cell Calcium. 2000; 28:285–296. [PubMed: 11115368]

Heeman B, Van den Haute C, Aelvoet SA, Valsecchi F, Rodenburg RJ, Reumers V, Debyser Z, Callewaert G, Koopman WJ, Willems PH, Baekelandt V. Depletion of PINK1 affects mitochondrial metabolism, calcium homeostasis and energy maintenance. J Cell Sci. 2011; 124:1115–1125. [PubMed: 21385841]

Jaiswal MK, Zech WD, Goos M, Leutbecher C, Ferri A, Zippelius A, Carri MT, Nau R, Keller BU. Impairment of mitochondrial calcium handling in a mtSOD1 cell culture model of motoneuron disease. BMC Neurosci. 2009; 10:64. [PubMed: 19545440]

Lefkimmiatis K, Leronni D, Hofer AM. The inner and outer compartments of mitochondria are sites of distinct cAMP/PKA signaling dynamics. J Cell Biol. 2013; 202:453–462. [PubMed: 23897891]

Martin MC, Allan LA, Lickrish M, Sampson C, Morrice N, Clarke PR. Protein kinase A regulates caspase-9 activation by Apaf-1 downstream of cytochrome c. J Biol Chem. 2005; 280:15449–15455. [PubMed: 15703181]

Neuberger G, Schneider G, Eisenhaber F. pkaPS: prediction of protein kinase A phosphorylation sites with the simplified kinase-substrate binding model. Biol Direct. 2007; 2:1. [PubMed: 17222345]

Nicholls DG, Budd SL. Mitochondria and neuronal survival. Physiol Rev. 2000; 80:315–360. [PubMed: 10617771]

Nicoll DA, Ottolia M, Goldhaber JI, Philipson KD. 20 years from NCX purification and cloning: milestones. Adv Exp Med Biol. 2013; 961:17–23. [PubMed: 23224866]

Nita II, Hershfinkel M, Fishman D, Ozeri E, Rutter GA, Sensi SL, Khananshvili D, Lewis EC, Sekler I. The mitochondrial Na^+/Ca^{2+} exchanger upregulates glucose dependent Ca^{2+} signalling linked to insulin secretion. PLoS ONE. 2012; 7:e46649. [PubMed: 23056385]

Obenauer JC, Cantley LC, Yaffe MB. Scansite 2.0: proteomewide prediction of cell signaling interactions using short sequence motifs. Nucleic Acids Res. 2003; 31:3635–3641. [PubMed: 12824383]

Palty R, Ohana E, Hershfinkel M, Volokita M, Elgazar V, Beharier O, Silverman WF, Argaman M, Sekler I. Lithium-calcium exchange is mediated by a distinct potassium-independent sodium-calcium exchanger. J Biol Chem. 2004; 279:25234–25240. [PubMed: 15060069]

Palty R, Silverman WF, Hershfinkel M, Caporale T, Sensi SL, Parnis J, Nolte C, Fishman D, Shoshan-Barmatz V, Herrmann S, et al. NCLX is an essential component of mitochondrial Na^+/Ca^{2+} exchange. Proc Natl Acad Sci USA. 2010; 107:436–441. [PubMed: 20018762]

Rakovic A, Grünewald A, Voges L, Hofmann S, Orolicki S, Lohmann K, Klein C. PINK1-interacting proteins: proteomic analysis of overexpressed PINK1. Parkinsons Dis. 2011; 2011:153979. [PubMed: 21437181]

Surmeier DJ, Schumacker PT. Calcium, bioenergetics, and neuronal vulnerability in Parkinson's disease. J Biol Chem. 2013; 288:10736–10741. [PubMed: 23086948]

Surmeier DJ, Guzman JN, Sanchez J, Schumacker PT. Physiological phenotype and vulnerability in Parkinson's disease. Cold Spring Harb Perspect Med. 2012; 2:a009290. [PubMed: 22762023]

Technikova-Dobrova Z, Sardanelli AM, Speranza F, Scacco S, Signorile A, Lorusso V, Papa S. Cyclic adenosine monophosphate-dependent phosphorylation of mammalian mitochondrial proteins: enzyme and substrate characterization and functional role. Biochemistry. 2001; 40:13941–13947. [PubMed: 11705384]

Valente EM, Abou-Sleiman PM, Caputo V, Muqit MM, Harvey K, Gispert S, Ali Z, Del Turco D, Bentivoglio AR, Healy DG, et al. Hereditary early-onset Parkinson's disease caused by mutations in PINK1. Science. 2004; 304:1158–1160. [PubMed: 15087508]

Valsecchi F, Ramos-Espiritu LS, Buck J, Levin LR, Manfredi G. cAMP and mitochondria. Physiology (Bethesda). 2013; 28:199–209. [PubMed: 23636265]

Vergun O, Reynolds IJ. Distinct characteristics of Ca(2+)-induced depolarization of isolated brain and liver mitochondria. Biochim Biophys Acta. 2005; 1709:127–137. [PubMed: 16112074]

von Heijne G. Membrane protein structure prediction. Hydrophobicity analysis and the positive-inside rule. J Mol Biol. 1992; 225:487–494. [PubMed: 1593632]

Wood-Kaczmar A, Gandhi S, Yao Z, Abramov AY, Miljan EA, Keen G, Stanyer L, Hargreaves I, Klupsch K, Deas E, et al. PINK1 is necessary for long term survival and mitochondrial function in human dopaminergic neurons. PLoS ONE. 2008; 3:e2455. [PubMed: 18560593]

Highlights

- Loss of PINK1 inhibits Ca^{2+} efflux by NCLX and triggers mitochondrial depolarization
- PKA prevents mitochondrial Ca^{2+} overload and depolarization by phosphorylating NCLX
- Phosphorylation of NCLX protects against dopaminergic neuron loss

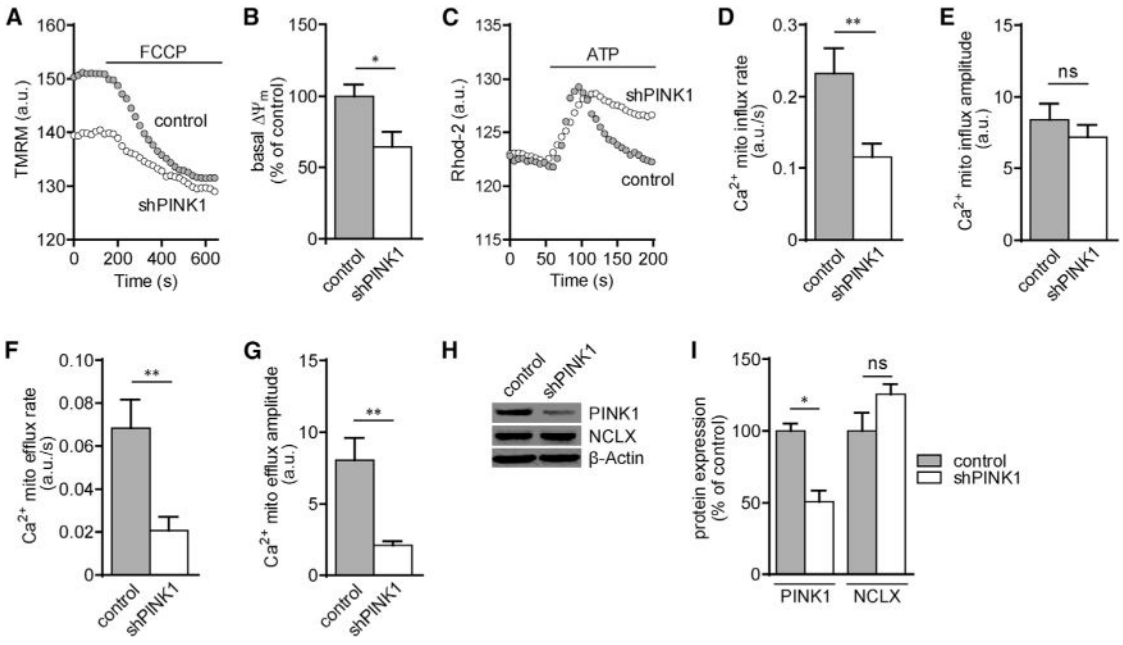

Figure 1. PINK1 Knockdown Triggers Mitochondrial Depolarization and Reduces $_{m}Ca^{2+}$ Efflux

(A) Representative fluorescence traces of ΔΨm determined in PINK1 knockdown SH-SY5Y cells (shPINK1) and control cells loaded and continuously superfused with TMRM (25 nM). FCCP (1 μM) was used to calibrate the signal by inducing a complete depolarization.

(B) Quantification of the resting ΔΨm of (A); shPINK1 cells (n = 5) show a reduction in basal ΔΨm compared to control cells (n = 9).

(C) Representative ATP-dependent fluorescence traces of $_{m}Ca^{2+}$ responses in shPINK1 cells versus control cells loaded with Rhod-2 AM (5 μM).

(D and E) Averaged rate and amplitude of the $_{m}Ca^{2+}$ influx phase of (C) (n = 13 and n = 10 for shPINK1 and control cells, respectively).

(F and G) Averaged rate and amplitude of the $_{m}Ca^{2+}$ efflux phase of (C) (n = 13 and n = 10 for shPINK1 and control cells, respectively). Note that PINK1 silencing in SH-SY5Y cells has a larger effect on both the rate and amplitude of the $_{m}Ca^{2+}$ efflux than the $_{m}Ca^{2+}$ influx phase.

(H and I) Immunoblot analysis of shPINK1 cells (n = 3) shows a similar level of NCLX expression compared to control cells (n = 3). Actin was used as a loading control. All bar graph data represent mean ± SEM. *p < 0.05, **p < 0.01; ns, not significant. See also Figure S1.

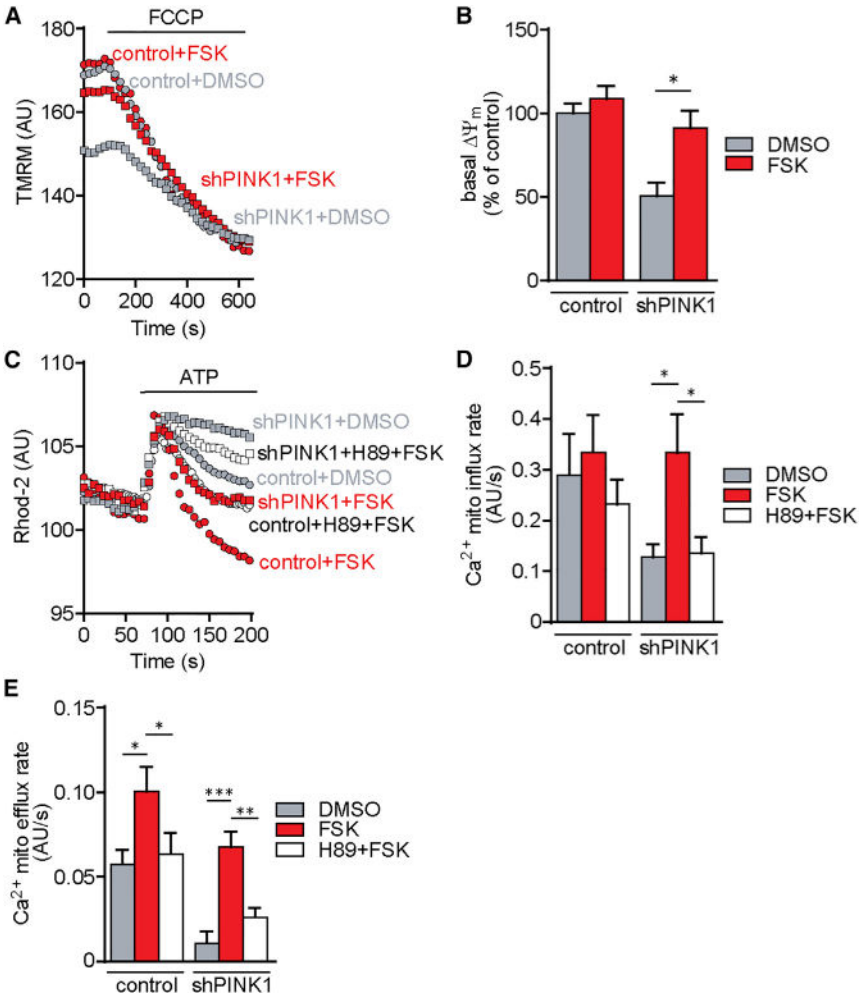

Figure 2. PKA Activation Rescues ΔΨm and Ca^{2+} Efflux in PINK1-Deficient Cells

(A) Representative fluorescence traces of ΔΨm determined in shPINK1 and control cells loaded and continuously superfused with TMRM in the presence or absence of the pharmacological activator of PKA, forskolin (FSK). FCCP induced complete depolarization and was used to calibrate the signal.

(B) Quantification of resting ΔΨm in shPINK1 (n = 6) and control cells (n = 4) treated with vehicle (DMSO) versus forskolin (50 μM, 2 hr). Significant repolarization of mitochondria was recorded in shPINK1 cells upon forskolin treatment.

(C) Representative fluorescence traces of $_{m}Ca^{2+}$ responses in Rhod-2 AM-loaded shPINK1 and control cells following application of ATP (100 μM). Cells were pretreated either with vehicle (DMSO), forskolin (50 μM, 15 min), or forskolin upon exposure to the PKA inhibitor H89 (10 μM, 1 hr).

(D and E) Averaged rates of the $_{m}Ca^{2+}$ influx and efflux phases of Figure 3C, respectively. Forskolin fully recovered both $_{m}Ca^{2+}$ influx and efflux in shPINK1 cells (n = 7) to control values; H89 fully prevented the activation of Ca^{2+} efflux by forskolin in shPINK1 cells (n = 9). Forskolin treatment in control cells (n = 5) increased only the rate of $_{m}Ca^{2+}$ efflux; this effect was prevented by pretreating the control cells with H89 as well (n = 3). All bar graph data represent mean ± SEM. *p < 0.05, **p < 0.01, ***p < 0.001.

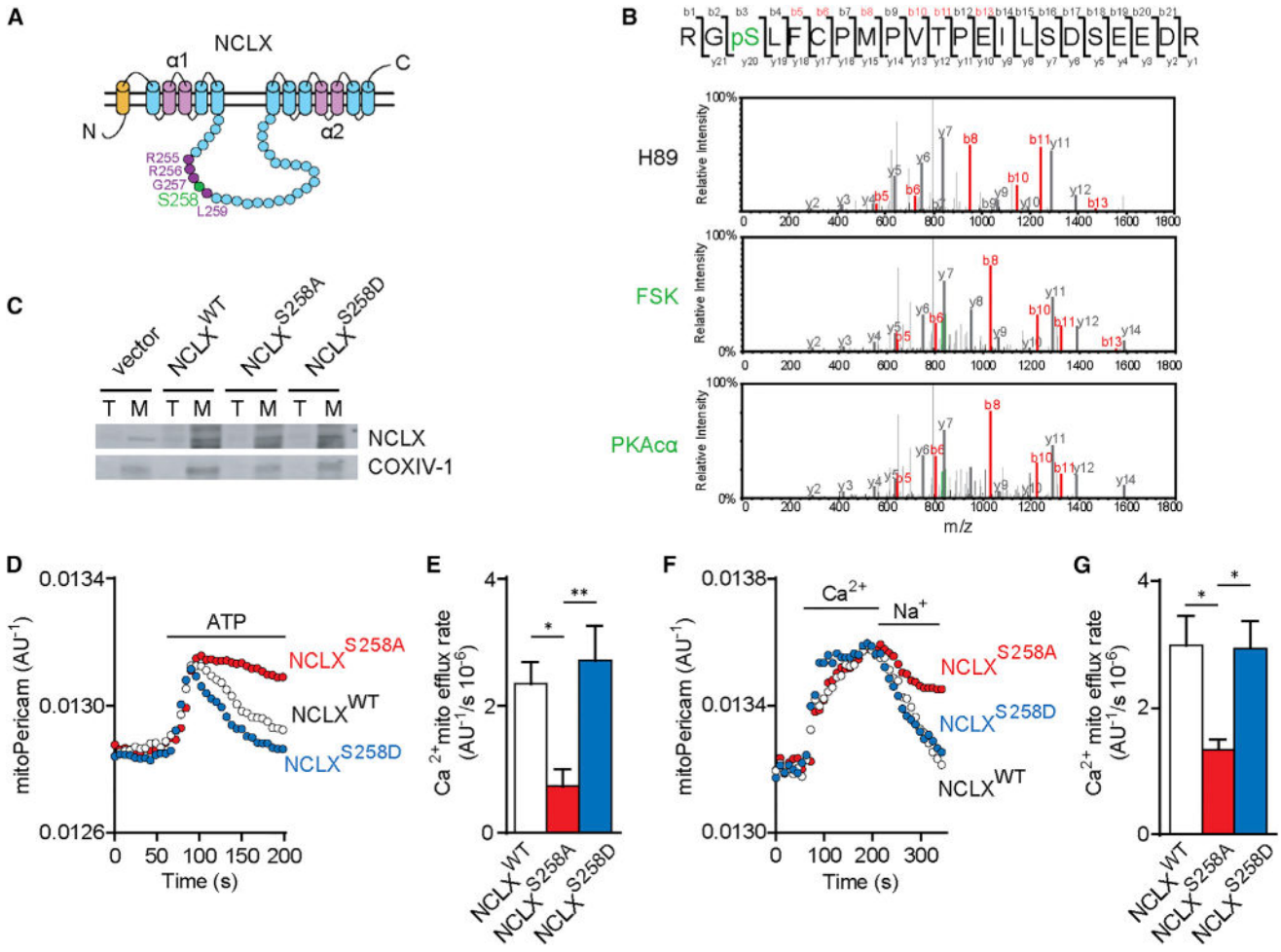

Figure 3. PKA Activates $_{m}Ca^{2+}$ Efflux through a Phosphorylation Site on NCLX

(A) The putative transmembrane topology model of NCLX obtained using TopPred (von Heijne, 1992). NCLX contains an N-terminal mitochondrial targeting sequence and two conserved catalytic transmembrane domains, α1 and α2. The putative PKA phosphorylation site Ser258 is located in the hydrophilic loop of the exchanger and is part of the PKA consensus sequence.

(B) Collision-induced dissociation MS/MS spectrum of the phosphorylated NCLX peptide $_{256}$RGpSLFCPMPVTPEILSDSEEDR$_{277}$ (where p indicates phosphorylation of S258) found only in c-*myc*-tagged NCLX isolated from cells treated with the PKA activator forskolin (middle panel) or following direct in vitro incubation with a recombinant PKA catalytic subunit (PKAcα) (lower panel) but not in the presence of the PKA inhibitor H89 (upper panel). *m/z*, mass-tocharge ratio. b_n and y_n denote N- and C-terminal fragments, respectively. Fragment ions that contain a mass shift as a result of phosphorylation are marked in red.

(C) Immunoblot analysis of NCLX expression in total lysate (T) and isolated mitochondria (M) in HEK293T cells transfected with either NCLX^{WT}-, NCLX^{S258A}-, or NCLX^{S258D}-coding plasmids or empty vector (pcDNA3.1+). COXIV-1 was used as a mitochondrial marker. NCLX is identified as a 100-kDa dimer in the mitochondrial fraction. Similar to

$NCLX_{WT}$, overexpression of the constructs $NCLX^{S258A}$ and $NCLX^{S258D}$ results in mitochondrial targeted expression, and NCLX expression is not affected by the mutation.
(D) Representative fluorescence traces of $_{m}Ca^{2+}$ responses upon application of ATP to HEK293T cells transiently expressing the $_{m}Ca^{2+}$ sensor mito-Pericam, NCLX shRNA, and $NCLX^{WT}$ or mutant NCLX ($NCLX^{S258A}$ or $NCLX^{S258D}$).
(E) Quantification of $_{m}Ca^{2+}$ efflux rates of (D). $NCLX^{S258D}$ (n = 10) and $NCLX^{WT}$ (n = 5) are ~3.5- and ~3-fold faster than $NCLX^{S258A}$ (n = 11), respectively.
(F) Representative fluorescence traces of Na^{+}-dependent $_{m}Ca^{2+}$ efflux in digitonin-permeabilized HEK293T cells transiently expressing the $_{m}Ca^{2+}$ sensor mito-Pericam, NCLX shRNA, and $NCLX^{WT}$ or mutant NCLX ($NCLX^{S258A}$ or $NCLX^{S258D}$).
(G) Quantification of $_{m}Ca^{2+}$ efflux rates of (F). Similar to Figure 3E, $NCLX^{S258D}$ (n = 3) and $NCLX^{WT}$ (n = 6) are more than 2-fold faster than $NCLX^{S258A}$ (n = 4). All bar graph data represent mean ± SEM. *$p < 0.05$, **$p < 0.01$. See also Figure S2 and Table S1.

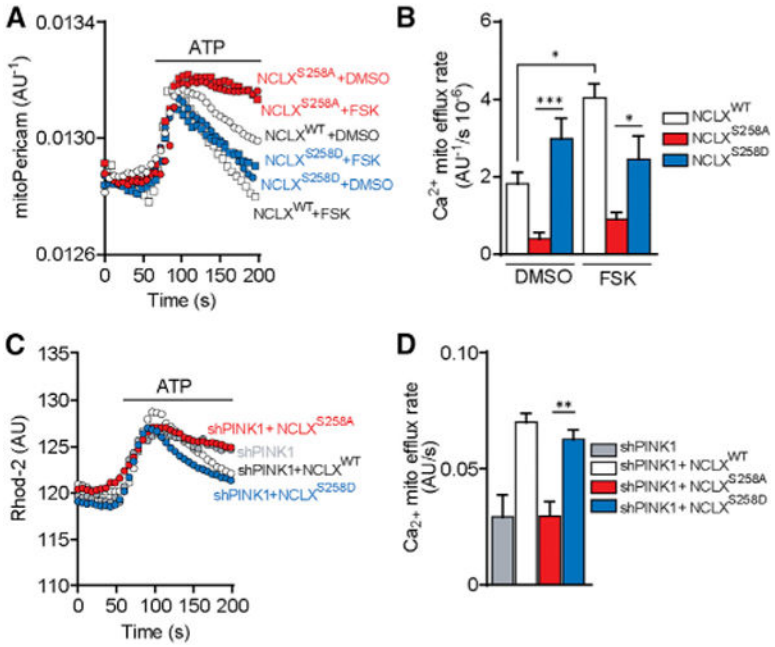

Figure 4. Phosphomimetic Mutants of NCLX Rescue $_{m}Ca^{2+}$ Homeostasis in PINK1-Deficient Cells Independent of PKA

(A) Representative fluorescence traces of $_{m}Ca^{2+}$ responses upon application of ATP to HEK293T cells transiently expressing the $_{m}Ca^{2+}$ sensor mito-Pericam, NCLX shRNA, and $NCLX^{WT}$ or mutant NCLX ($NCLX^{S258A}$ or $NCLX^{S258D}$) in the absence or presence of forskolin.

(B) Averaged rates of $_{m}Ca^{2+}$ efflux of data in (A). A minimum of n = 5 independent experiments for all quantified data. Note that the mutants $NCLX^{S258A}$ and $NCLX^{S258D}$, unlike $NCLX^{WT}$, are not responsive to forskolin.

(C) Representative fluorescence traces of $_{m}Ca^{2+}$ responses in shPINK1 SH-SY5Y cells overexpressing $NCLX^{WT}$, $NCLX^{S258A}$, and $NCLX^{S258D}$, or nontransfected shPINK1 SH-SY5Y cells loaded with 5 μM Rhod-2 AM. Application of 100 μM ATP triggered $_{m}Ca^{2+}$ transients.

(D) Averaged $_{m}Ca^{2+}$ efflux rates of (C). Constitutively active mutant $NCLX^{S258D}$ (n = 9) and $NCLX^{WT}$ (n = 3), in contrast to inactive $NCLX^{S258A}$ (n = 9), are able to overcome the inhibitory effect of PINK1 deficiency on $_{m}Ca^{2+}$ removal. All bar graph data represent mean ± SEM. *$p < 0.05$, **$p < 0.01$, ***$p < 0.001$.

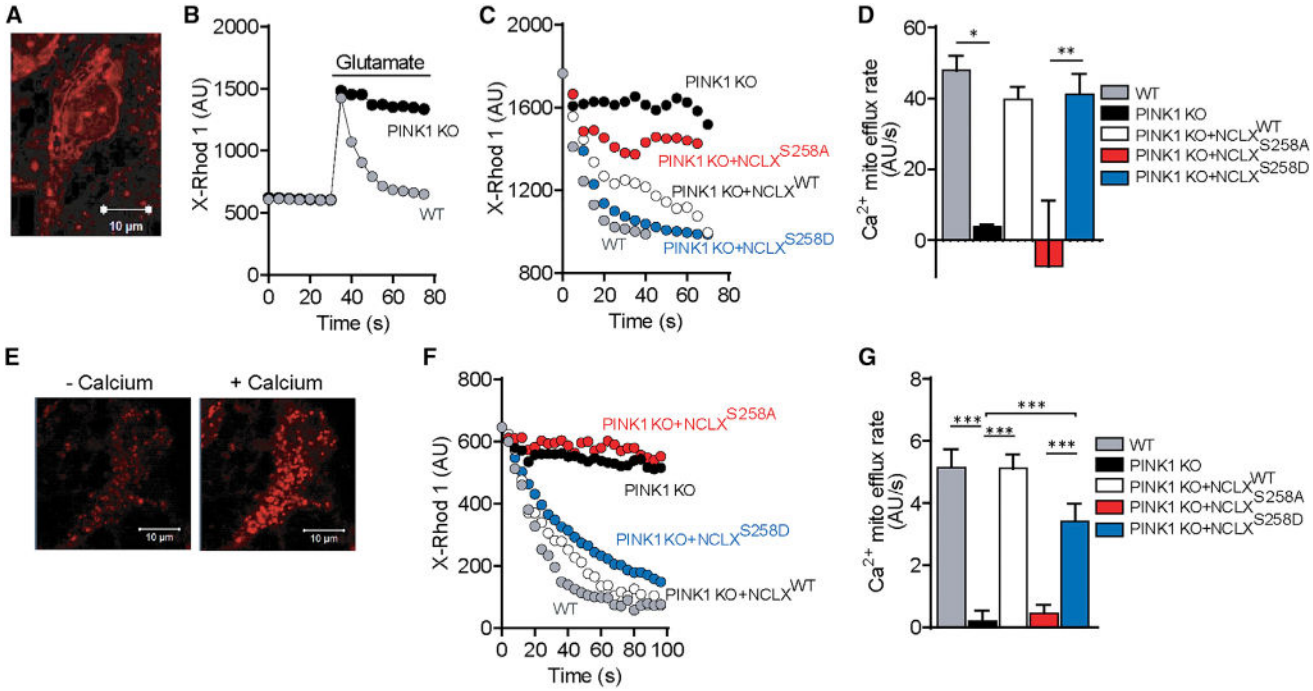

Figure 5. Phosphomimetic Mutant NCLX^{S258D}, in Contrast to Phosphodeficient NCLX^{S258A}, Rescues $_{m}Ca^{2+}$ Efflux in PINK1 KO Neurons

(A) Image of a whole neuron loaded with X-Rhod-1 AM. The scale bar represents 10 μm.

(B) Representative traces of $_{m}Ca^{2+}$ response upon glutamate stimulation in intact neurons. Note the inhibition of $_{m}Ca^{2+}$ efflux in PINK1 KO neurons compared to WT neurons.

(C and D) Representative traces and quantification of the $_{m}Ca^{2+}$ efflux upon glutamate stimulation in intact WT (n = 11), PINK1 KO (n = 3), or PINK1 KO neurons overexpressing either NCLX^{S258A} (n = 4), NCLX^{S258D} (n = 4), or NCLX^{WT} (n = 11).

(E) Images of permeabilized neurons that were loaded with X-Rhod-1 before and after Ca^{2+} stimulation. The scale bars represent 10 μm.

(F and G) Representative traces and quantification of $_{m}Ca^{2+}$ efflux upon Ca^{2+} stimulation in permeabilized PINK1 KO neurons (n = 9) and PINK1 KO neurons overexpressing NCLX^{WT} (n = 7), NCLX^{S258A} (n = 11), or NCLX^{S258D} (n = 6), respectively. All bar graph data represent mean ± SEM. *p < 0.05, **p < 0.01, ***p < 0.001. See also Figure S3.

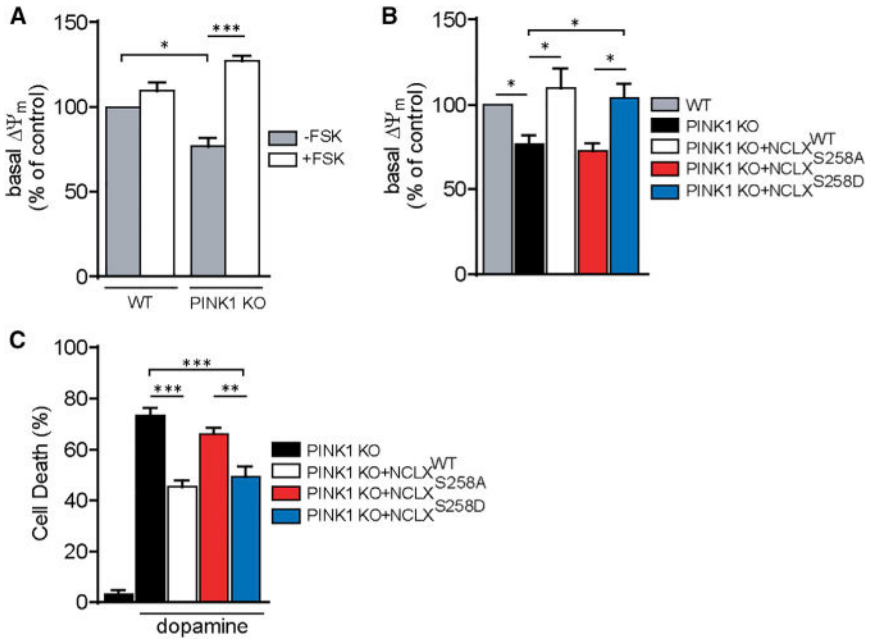

Figure 6. NCLX^{S258D} Overexpression Restores ΔΨm in PINK1 KO Neurons and Rescues Them from Dopamine-Induced Cell Death

(A) Quantification of basal ΔΨm in WT (n = 6) and PINK1 KO (n = 16) neurons in the absence and presence of forskolin. Note that forskolin treatment reduces mitochondrial depolarization of PINK1 KO neurons to control values.

(B) Quantification of basal ΔΨm in WT neurons (n = 6), PINK1 KO neurons (n = 22), and PINK1 KO neurons overexpressing NCLX^{WT} (n = 9), constitutively active NCLX^{S258D} (n = 6), and inactive NCLX^{S258A} (n = 4) constructs.

(C) Quantification of dopamine-induced cell death in PINK1 KO neurons (n = 12) and PINK1 KO neurons overexpressing NCLX^{WT} (n = 10), constitutively active NCLX^{S258D} (n = 9), and inactive NCLX^{S258A} (n = 13) constructs. All bar graph data represent mean ± SEM. *p < 0.05, **p < 0.01, ***p < 0.001

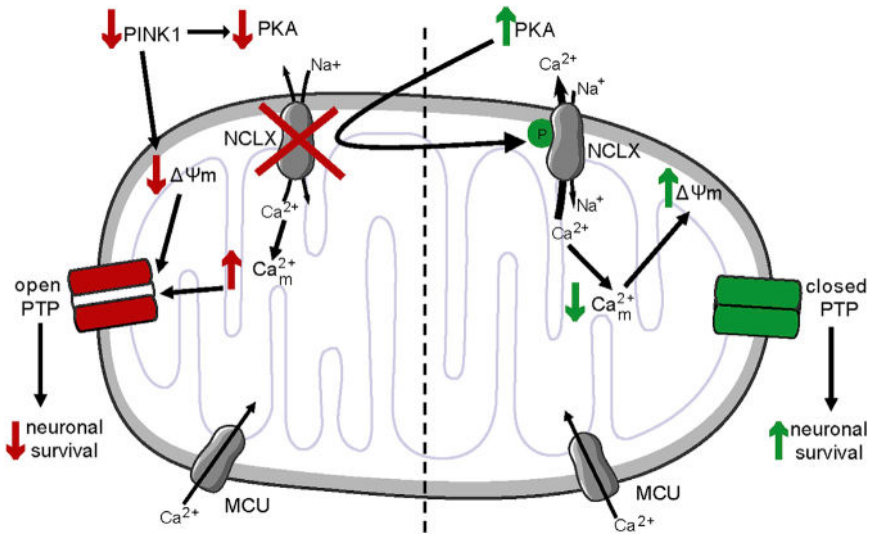

Figure 7. Schematic Diagram Illustrating the Link between PINK1 Deficiency and PKA-Mediated Rescue of $_{m}Ca^{2+}$ Dyshomeostasis and Ultimately Neuronal Fate

PINK1 deficiency leads to mitochondrial damage and depolarization, leading to inhibition of the Na+/Ca^{2+} exchanger NCLX, the major Ca^{2+} efflux pathway in mitochondria. The resulting buildup of $_{m}Ca^{2+}$ overload, combined with mitochondrial depolarization, can result in the opening of the mitochondrial permeability transition pore. PKA independent of PINK1 activates NCLX via phosphorylation at S258. Phosphorylation of NCLX rescues its activity in PINK1-deficient neurons and stops this vicious cycle, leading to recovery of mitochondrial membrane potential, thus enhancing dopaminergic neuronal survival.